Synthesis, Characterization, and Structure of $(\eta^5\text{-}C_9H_7)_3Ir_3(\mu\text{-}CO)_3$. Comparative Spectroscopic Properties of $(\eta^5\text{-}C_9H_7)_3Ir_{3-x}Rh_x(\mu\text{-}CO)_3$ ($x = 0-3$)

Matthew C. Comstock, Scott R. Wilson, and John R. Shapley*

School of Chemical Sciences, University of Illinois, Urbana, Illinois 61801

Received April 21, 1994[⊗]

The triiridium cluster $(\eta^5\text{-}C_9H_7)_3Ir_3(\mu\text{-}CO)_3$, **1**, has been prepared from the reaction of $(\eta^5\text{-}C_9H_7)Ir(CO)_2$ with $(\eta^5\text{-}C_9H_7)Ir(\eta^2\text{-}C_2H_4)_2$ in 74% yield. The compound crystallizes in the monoclinic space group $P2_1/c$, with $a = 9.392(2)$, $b = 14.765(3)$, $c = 18.038(7)$ Å, $\beta = 104.83(2)°$ and $Z = 4$, and its structure was solved with conventional procedures and refined to $R = 0.031$ and $R_w = 0.031$. The molecular structure of **1** shows approximate C_{3v} symmetry and consists of a triangle of iridium atoms, each edge of which has a bridging carbonyl oriented out of the plane in the same direction, and each vertex of which has a slightly "slipped" η^5-indenyl ligand oriented toward the opposite of the plane. The proton NMR and infrared spectra of **1** are consistent with the solid state structure. The reaction of $(\eta^5\text{-}C_9H_7)Ir(CO)_2$ with $(\eta^5\text{-}C_9H_7)Rh(\eta^2\text{-}C_2H_4)_2$ gave all four possible trinuclear products $(\eta^5\text{-}C_9H_7)_3Ir_{3-x}Rh_x(\mu\text{-}CO)_3$ ($x = 0$, **1**; $x = 1$, **2**; $x = 2$, **3**; $x = 3$, **4**), which have been separated and characterized. The reactions of **1**–**4** with CO at room temperature led to immediate formation of $(\eta^5\text{-}C_9H_7)M(CO)_2$ (M = Ir, Rh).

Trinuclear compounds of the cobalt triad with the general formula $(\eta^5\text{-}L)_3M_3(CO)_3$, where L refers to $\eta^5\text{-}C_5H_5$ and related ligands, have been observed to adopt geometries A–D (see Table 1).[1]

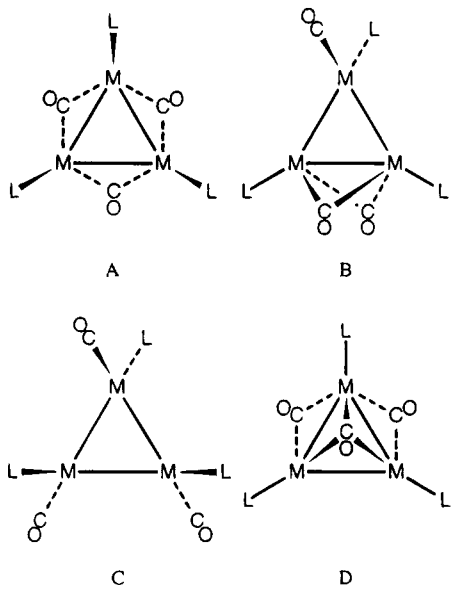

The reactions of $(\eta^5\text{-}C_5R_5)M(CO)_2$ with $(\eta^5\text{-}C_5R_5)M(\eta^2\text{-}C_2H_4)_2$ (R = H, Me; M = Co, Rh, Ir) result in formation of a variety of di- and trinuclear compounds.[2] The analogous reaction in the indenyl-iridium system was reported to lead to formation of the saturated dinuclear species $(\eta^5\text{-}C_9H_7)_2Ir_2(\mu\text{-}CO)(CO)_2$.[3] Our reinvestigation of the reaction of $(\eta^5\text{-}C_9H_7)Ir(CO)_2$ with $(\eta^5\text{-}C_9H_7)Ir(\eta^2\text{-}C_2H_4)_2$ has resulted in the isolation and characterization of a new trinuclear compound, $(\eta^5\text{-}C_9H_7)_3Ir_3(\mu\text{-}CO)_3$ (**1**).

In the attempt to prepare the corresponding mixed-metal clusters, we have also explored the reaction of $(\eta^5\text{-}C_9H_7)Ir(CO)_2$ with $(\eta^5\text{-}C_9H_7)Rh(\eta^2\text{-}C_2H_4)_2$. Separation of the reaction mixture has provided four trinuclear clusters with metal compositions Ir_3, **1**; $RhIr_2$, **2**; $IrRh_2$, **3**; and Rh_3, **4** (see Scheme 1). The synthesis and characterization of **4**, prepared by a different method, has been reported previously.[1g,h]

Table 1. Geometries of Trinuclear Compounds with the Formula $(\eta^5\text{-}L)_3M_3(CO)_3$

metals	ligands[a]	structures[b]	ref
Co_3	Cp_3	B, D[c]	1a
	MeCp, Cp^*_2	D	1b
	$MeCp_3$	B	1a
Rh_3	Cp_3	A, B[d]	1c–e
	Cp^*_3	D[e]	1f
	Ind_3	A[e]	1g,h
$IrRh_2$	Ind_3	A[e]	this work
$RhIr_2$	Ind_3	A[e]	this work
Ir3	Cp_3	C	1i
	Ind_3	A	this work
$IrCo_2$	Cp*, Cp_2	A	1j

[a] Cp = $\eta^5\text{-}C_5H_5$, MeCp = $\eta^5\text{-}C_5H_4Me$, Cp* = $\eta^5\text{-}C_5Me_5$, Ind = $\eta^5\text{-}C_9H_7$. [b] See text. [c] Structure D is observed in the solid state, while B is observed in solution. [d] A and B isomers can be isolated separately but can be interconverted. [e] Structure deduced by infrared and NMR spectroscopy.

Results and Discussion

Syntheses and Characterization of Trinuclear Clusters 1–4. Heating a 1:1 mixture of $(\eta^5\text{-}C_9H_7)Ir$-

[⊗] Abstract published in *Advance ACS Abstracts,* August 1, 1994.

(1) (a) Cotton, F. A.; Jamerson, J. D. *J. Am. Chem. Soc.* **1976**, *98*, 1273. (b) Cirjak, L. M.; Huang, J.-S.; Zhu, Z.-H.; Dahl, L. F. *J. Am. Chem. Soc.* **1980**, *102*, 6623. (c) Paulus, E. F.; Fischer, E. O.; Fritz, H. P.; Schuster-Woldan, H. *J. Organomet. Chem.*, **1967**, *10*, P3. (d) Paulus, E. F. *Acta Crystallogr., Sect. B* **1969**, *25*, 2206. (e) Mills, O. S.; Paulus, E. F. *J. Organomet. Chem.* **1967**, *10*, 331. (f) Aldridge, M. L.; Green, M.; Howard, J. A. K.; Pain, G. N.; Porter, S. J.; Stone, F. G. A.; Woodward, P. *J. Chem. Soc., Dalton Trans.* **1982**, 1333. (g) Caddy, P.; Green, M.; O'Brien, E.; Smart, L. E.; Woodward, P. *Angew. Chem., Int. Ed. Engl.* **1977**, *16*, 648. (h) Al-Obaidi, Y. N.; Green, M.; White, N. D.; Taylor, G. E. *J. Chem. Soc., Dalton Trans.* **1982**, 319. (i) Shapley, J. R.; Adair, P. C.; Lawson, R. J.; Pierpont, C. G. *Inorg. Chem.* **1982**, *21*, 1701. (j) Hörlein, R.; Herrmann, W. A.; Barnes, C. E.; Weber, C.; Kruger, C.; Ziegler, M. L.; Zahn, T. *J. Organomet. Chem.* **1987**, *321*, 257.

(2) Barnes, C. E.; Dial, M. R.; Orvis, J. A.; Staley, D. L.; Rheingold, A. L. *Organometallics* **1990**, *9*, 1021; and references therein.

(3) Abad, J. A. *Inorg. Chim. Acta.* **1986**, *121*, 213.

0276-7333/94/2313-3805$04.50/0

Scheme 1

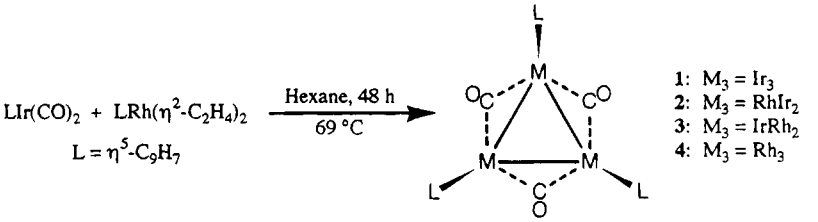

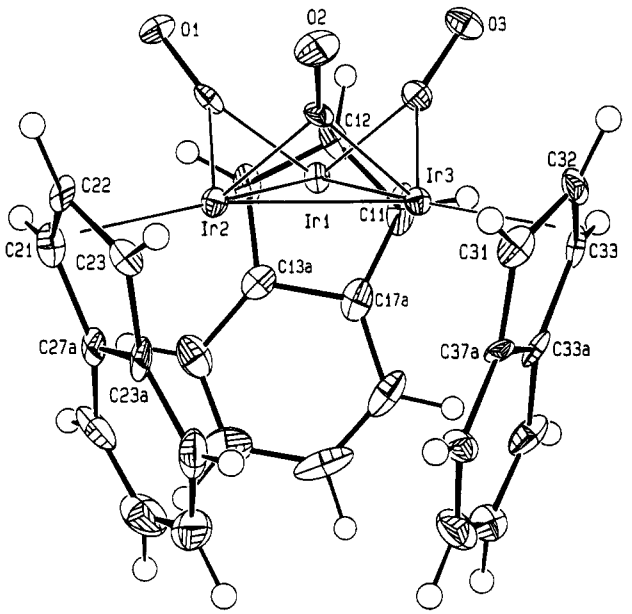

Figure 1.

Table 2. Crystallographic Data for (η^5-C_9H_7)$_3$Ir$_3$(μ-CO)$_3$ (1)

formula	$C_{30}H_{21}O_3Ir_3$	λ	0.71073 Å (Mo Kα)
fw	1006.16	ϱ_{calcd}	2.764 g/cm^3
temp	−50 °C	μ	164.49 cm^{-1}
size	0.04 × 0.10 × 0.38 mm	transm coeff	0.558−0.176
space grp	$P2_1/c$, monoclinic	$2\theta_{max}$ (octs)	32° ($\pm h,\pm k,\pm l$)
a	9.392(2) Å	I_{tot} (unique, R_i)	4216 (3795, 0.022)
b	14.765(3) Å	$I > 2.58\sigma(I)$	2731
c	18.038(7) Å	final ΔF map	+1.12 > e/Å^3 > −1.08
$\alpha = \gamma, \beta$	90°, 104.83(2)°	R^a	0.031
V	2418(16) Å^3	$R_w{}^b$	0.031

^{a} $R = \sum||F_o| - |F_c||/\sum|F_o|$. ^{b} $R_w = [|\sum w(|F_o| - |F_c|)^2/\sum w|F_o|^2]^{1/2}$; $w = k/([\sigma(F_o)]^2 + [pF_o]^2)$, $k = 1.46$, $p = 0.01$.

$(CO)_2$ and (η^5-C_9H_7)Ir(η^2-C_2H_4)$_2$ in hexane at reflux results in the slow precipitation of red, solid (η^5-C_9H_7)$_3$-Ir$_3$(μ-CO)$_3$ (74%; 97% based on unrecovered starting materials). The starting materials remaining are easily quantified by bubbling a stream of CO through the supernatant solution for 15 min to convert all reagents to (η^5-C_9H_7)Ir(CO)$_2$, followed by IR determination.

Heating a one-to-one mixture of (η^5-C_9H_7)Ir(CO)$_2$ and (η^5-C_9H_7)Rh(η^2-C_2H_4)$_2$ in hexane at reflux results in the formation of trinuclear clusters **1**−**4**. Any remaining starting materials are converted to (η^5-C_9H_7)M(CO)$_2$ (M = Ir, Rh), and quantified as described above. The clusters **1**−**4** were separated by column chromatography and isolated in 2:7:5:1 molar ratios with 99% yield of Ir and 79% yield of Rh overall (incorporated into **1**−**4**) based on unrecovered starting materials.

During the reaction to form **1**, (η^5-C_9H_7)$_2$Ir$_2$(μ-CO)-(CO)$_2$ was identified by peaks in the infrared spectrum at 1973 and 1814 cm^{-1}.[3] A sample of this dinuclear species was examined by proton NMR. At 20 °C the

Table 3. Positional Parameters for (η^5-C_9H_7)$_3$Ir$_3$(μ-CO)$_3$ (1)

atom	*x/a*	*y/b*	*z/c*
Ir1	0.48636(6)	0.23367(3)	0.96744(3)
Ir2	0.23986(6)	0.33254(3)	0.94100(3)
Ir3	0.22274(6)	0.15286(3)	0.92766(3)
O1	0.463(1)	0.3690(6)	1.0874(5)
O2	0.060(1)	0.2380(6)	1.0305(5)
O3	0.432(1)	0.0886(6)	1.0695(5)
C1	0.416(1)	0.3280(7)	1.0288(8)
C2	0.140(1)	0.2382(7)	0.9905(7)
C3	0.395(2)	0.1386(8)	1.0161(8)
C11	0.663(2)	0.1482(8)	0.9475(10)
C12	0.720(1)	0.2066(8)	1.0106(9)
C13	0.705(1)	0.2947(8)	0.9808(8)
C13a	0.666(1)	0.2921(8)	0.8999(8)
C14	0.646(2)	0.3595(9)	0.8440(10)
C15	0.607(2)	0.335(1)	0.769(1)
C16	0.584(2)	0.245(1)	0.7477(10)
C17	0.596(2)	0.178(1)	0.799(1)
C17a	0.637(2)	0.1993(9)	0.8775(9)
C21	0.266(2)	0.4788(8)	0.9215(9)
C22	0.143(2)	0.4627(7)	0.9505(8)
C23	0.037(1)	0.4124(7)	0.8958(7)
C23a	0.086(2)	0.4078(7)	0.8254(9)
C24	0.025(2)	0.3709(8)	0.753(1)
C25	0.101(2)	0.3777(10)	0.6998(10)
C26	0.239(3)	0.418(1)	0.715(1)
C27	0.307(2)	0.4541(9)	0.785(1)
C27a	0.228(2)	0.4485(8)	0.8427(8)
C31	0.009(2)	0.0826(8)	0.8780(8)
C32	0.114(2)	0.0209(8)	0.9222(8)
C33	0.233(1)	0.0142(7)	0.8854(8)
C33a	0.189(2)	0.0590(8)	0.8110(8)
C34	0.251(2)	0.0673(9)	0.7491(9)
C35	0.172(2)	0.1134(9)	0.6855(9)
C36	0.035(2)	0.1491(9)	0.6819(9)
C37	−0.030(2)	0.1442(8)	0.7404(8)
C37a	0.046(2)	0.1006(8)	0.8070(7)

NMR spectrum exhibited only broad peaks in the range of indenyl protons, suggesting a dynamic process was occurring. At about −40 °C this fluxionality was frozen out, and a pattern of seven peaks, indicative of an indenyl ligand in an asymmetric environment, was observed.[4] This latter spectrum is consistent with the structure previously proposed for this species,[3] although no mention was made of this fluxional behavior.

Infrared spectra were obtained during the course of the reaction of (η^5-C_9H_7)Ir(CO)$_2$ with (η^5-C_9H_7)Rh(η^2-C_2H_4)$_2$ that suggested an intermediate of the form (η^5-C_9H_7)$_2$MRh(μ-CO)(CO)$_2$ (M = Ir or Rh) with peaks at 1989 and 1834 cm^{-1} (no peaks were observed corresponding to the diiridium compound described above). The dirhodium species, (η^5-C_9H_7)$_2$Rh$_2$(μ-CO)(CO)$_2$, was reported to exhibit peaks in the infrared spectrum at 1988 and 1846 cm^{-1} in hexane.[1h] While the higher frequency peaks in the infrared spectrum of a mixture of IrRh and Rh$_2$ species could overlap, the lower

(4) (η^5-C_9H_7)$_2$Ir$_2$(μ-CO)(CO)$_2$: ^{1}H NMR (CD_2Cl_2, −40 °C) δ 7.29 (m, 2H), 7.20 (m, 2H), 7.04 (m, 2H), 6.92 (m, 2H), 6.18 (m, 2H), 5.93 (m, 2H), 5.03 (m, 2H).

Table 4. Selected Bond Lengths (Å) and Angles (deg) for $(\eta^5\text{-}C_9H_7)_3Ir_3(\mu\text{-}CO)_3$ (1)

Bond Distances

Ir1–Ir2	2.6745(7)	Ir1–Ir3	2.6757(7)	Ir2–Ir3	2.6650(6)
Ir1–C1	1.99(1)	Ir2–C1	1.98(1)	O1–C1	1.20(2)
Ir2–C2	2.01(1)	Ir3–C2	1.98(1)	O2–C2	1.17(2)
Ir1–C3	1.96(1)	Ir3–C3	1.97(1)	O3–C3	1.19(2)
Ir1–C11	2.18(1)	Ir1–C12	2.17(1)	Ir1–C13	2.20(1)
Ir1–C13a	2.47(1)	Ir1–C17a	2.46(2)	Ir2–C21	2.21(1)
Ir2–C22	2.15(1)	Ir2–C23	2.21(1)	Ir2–C23a	2.47(1)
Ir2–C27a	2.45(1)	Ir3–C31	2.23(1)	Ir3–C32	2.19(1)
Ir3–C33	2.20(1)	Ir3–C33a	2.47(1)	Ir3–C37a	2.50(1)

Bond Angles

Ir1–Ir2–Ir3	60.15(2)	Ir2–Ir3–Ir1	60.10(2)	Ir3–Ir1–Ir2	59.75(2)
Ir1–Ir2–C1	47.9(3)	Ir2–Ir3–C2	48.6(3)	Ir3–Ir1–C3	47.3(4)
Ir2–Ir1–C1	47.4(4)	Ir3–Ir2–C2	47.6(3)	Ir1–Ir3–C3	47.1(4)
Ir1–C1–Ir2	84.7(5)	Ir2–C2–Ir3	83.8(5)	Ir3–C3–Ir1	85.6(5)

Interplanar Angles

Ir1, Ir2, Ir3 vs Ir1, Ir2, C1	52.55
Ir1, Ir2, Ir3 vs Ir2, Ir3, C2	56.04
Ir1, Ir2, Ir3 vs Ir1, Ir3, C3	56.02
Ir1, Ir2, Ir3 vs C11, C12, C13, C13a, C17a	75.09
Ir1, Ir2, Ir3 vs C21, C22, C23, C23a, C27a	74.47
Ir1, Ir2, Ir3 vs C31, C32, C33, C33a, C37a	76.75
C11, C12, C13 vs C13a, C14, C15, C16, C17, C17a	10.59
C21, C22, C23 vs C23a, C24, C25, C26, C27, C27a	7.42
C31, C32, C33 vs C33a, C34, C35, C36, C37, C37a	12.26

frequency peaks appear to be readily distinguishable, and the intermediate observed in our reaction is most likely the mixed-metal dinuclear species.

Structural Features. The molecular structure of **1** as determined by X-ray crystallography is shown in Figure 1. It consists of a triangular Ir_3 framework with three bridging carbonyls oriented toward one side of the triangle and three η^5-C_9H_7 ligands over the opposite side. The Ir–Ir distances in **1** are all similar at 2.672 ± 0.006 Å, so that the metal atoms form a nearly equilateral triangle (see Table 4). The degree of distortion in η^5-C_9H_7 complexes can be described by the slip distortion parameter, Δ, and the fold angle.[5] In compound **1**, the average slip distortion parameter for the three indenyl ligands is 0.27 Å and the average fold angle is 10.1° (e.g. for the indenyl ligand attached to Ir3, Δ = [average (Ir3–C33a, Ir3–C37a) − average (Ir3–C31, Ir3–C33)]; the fold angle = the angle between the planes defined by C31, C32, C33 and C33a, C34, C35, C36, C37, C37a). For comparison, the mononuclear indenyl–rhodium compound, $(\eta^5\text{-}C_9H_7)Rh(CO)_2$, has Δ = 0.20 Å and a fold angle of 10.9°.[6]

The structure of **1** contrasts in two respects with that of $Cp_3Ir_3(CO)_3$.[1i] First, the latter compound contains only terminal CO ligands, two on one side of the Ir_3 triangle and one on the other. Furthermore, the compound displays two different Ir–Ir distances, two nearly identical at 2.6693(7) and 2.6697(6) Å and one at 2.6876(6) Å, consistent with nearly mirror symmetry. For comparison, the tetrahedral cluster $Ir_4(CO)_{12}$ has an Ir–Ir distance of 2.693 Å.[7]

The infrared spectra of the trinuclear clusters **1**–**4** in dichloromethane solution show only bridging carbonyls present, but a distinct trend is observed as the metal composition is altered. With the replacement of iridium with rhodium, from cluster **1** to **4**, the peaks in the infrared spectra shift by a minimum of 10 cm^{-1} to higher frequency (Figure 2). The direction and magnitude of this trend is consistent with that observed in the mononuclear cases; the infrared spectrum of $(\eta^5\text{-}C_9H_7)M(CO)_2$ in light petroleum solution has peaks at 2042 and 1980 cm^{-1} for M = Ir[3] and at 2048 and 1990 cm^{-1} for M = Rh.[1g,h] Furthermore, the lower symmetry of **2** and **3** compared to **1** and **4** is reflected in the broadening of the lower energy band.

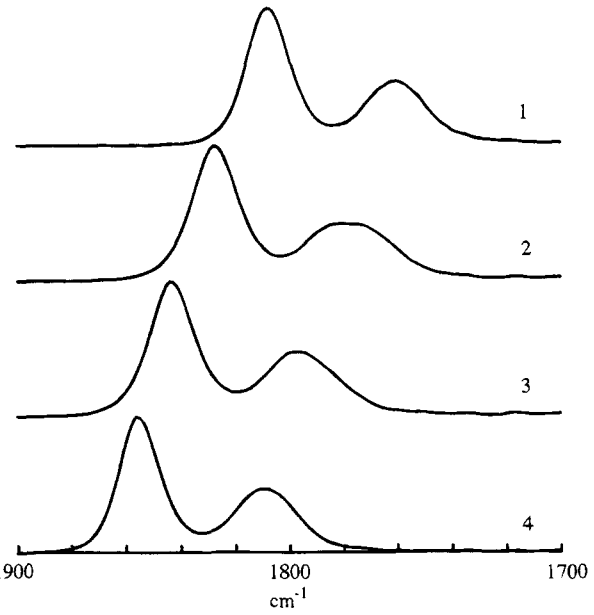

Figure 2.

Analysis of the intensities of the bands due to the symmetric (A_1) and degenerate antisymmetric (E) carbonyl stretches in a molecule exhibiting C_{3v} symmetry can provide insight into the molecular structure.[8] In particular, with the crystal structure of **1** available, a comparison of the predicted and observed values for the angles defining the CO bond vectors is possible. The angles of interest are those defined by the CO bond vectors with respect to the M_3 plane (ϕ). Using the bond vectors calculated from the C and O atomic coordinates, the observed values of ϕ were 48.3°, 51.2°, and 51.1° for an averaged value of 50.2°. The areas of the peaks in the infrared spectrum of **1** were determined by triangulation. The predicted value of ϕ was found to be 51.3° using the equation $I(A_1)/I(E) = \tan^2 \phi$, where $I(A_1)$ and I(E) are the intensities of the symmetric and the degenerate antisymmetric bands, respectively. This method was also applied to the spectrum of **4**, leading to a predicted value of ϕ as 47.8°.

The ^1H NMR spectra for **1** and **4** contained only four indenyl resonances while those for **2** and **3** were more complicated (see Table 5). The simple spectra for **1** and **4** require the chemical equivalence of all the indenyl ligands in each molecule as well as requiring that each indenyl ligand lies on a mirror plane. In contrast, the ^1H NMR spectra of **2** and **3** exhibit two sets of indenyl resonances in a two-to-one ratio with only the smaller set consistent with mirror symmetry. These spectra are

(5) (a) Faller, J. W.; Crabtree, R. H.; Habib, A. *Organometallics* **1985**, *4*, 929. (b) Baker, R. T.; Tulip, T. H. *Organometallics* **1986**, *5*, 839. (c) Donovan, B. T.; Hughes, R. P.; Trujillo, H. A.; Rheingold, A. L. *Organometallics* **1992**, *11*, 64.

(6) Kakkar, A. K.; Taylor, N. J.; Calabrese, J. C.; Nugent, W. A.; Roe, D. C.; Connaway, E. A.; Marder, T. B. *J. Chem. Soc., Chem. Commun.* **1989**, 990.

(7) Churchill, M. R.; Hutchinson, J. P. *Inorg. Chem.* **1978**, *17*, 3528.

(8) Braterman, P. S. *Metal Carbonyl Spectra*; Academic Press: London, 1975; Chapter 3.

Table 5. ^{1}H NMR Data for Compounds 1–4

		M(C$_9$H$_7$)[a]			
compound	M	H_2	H_1,H_3	J(Hz)	H_4–H_7[b]
1[c]	Ir	5.90t	5.55d	$J_{12} = 2.7$	7.14, 7.24
2[d]	Rh	6.00q	5.68d	$J_{12} = J_{RhH} = 2.9$	7.06–7.35
	Ir	5.78m	5.46m, 5.37m		
3[d]	Ir	5.38t	5.27d	$J_{12} = 2.7$	7.07–7.35
	Rh	5.93m	5.64m, 5.56m		
4[c,e]	Rh	5.64q	5.51d	$J_{12} = J_{RhH} = 2.9$	7.17, 7.27

[a] Spectra were recorded at 300 MHz, and chemical shifts are referenced to residual solvent protons. The labeling scheme was used for assignments. [b] The resonances for H_4–H_7 appear as AA′BB′ multiplets for **1** and **4** and as overlapping multiplets for **2** and **3**. [c] CD_2Cl_2, 20 °C. [d] $CDCl_3$, 20 °C. [e] See ref 1h for preparation and characterization.

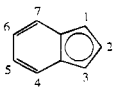

consistent with the expected C_s geometries, with a mirror plane perpendicular to the M_3 plane, and passing through the heterometal.

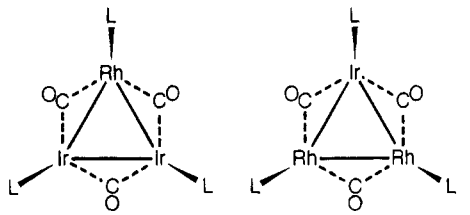

2 **3**

L = η^5-C$_9$H$_7$

Bonding and Reactivity. The UV-visible spectra of **1**–**4** each show a strong, low-energy absorption that decreases in energy on progression from **1** to **4** (Figure 3). These absorptions are undoubtedly due to transitions involving metal–metal bonding, as the corresponding mononuclear precursors do not absorb significantly above 400 nm. The red shift is consistent with decreasing strength of the metal–metal interactions as more rhodium is introduced into the trimetallic framework.

The bonding in triangular metal clusters has been discussed several times on the basis of various levels of theory.[9] The simplest analysis in terms of Walsh cyclopropane-like orbitals predicts the highest lying orbitals to be an a + e set containing the metal–metal bonding electrons. However, mixing with the CO π^* orbitals can complicate the nature of the valence orbitals; the HOMO for $Ru_3(CO)_{12}$ apparently has rather little d-orbital contribution.[10] In the absence of further spectroscopic data or guidance from calculations, we hesitate to speculate about band assignments. Nevertheless, the regular progression of λ_{max} for the lowest energy transitions certainly suggests a distinct metal–metal bonding to metal–metal antibonding (or $\sigma \rightarrow \sigma^*$) character.[11]

Treatment of solutions of **1**–**4** with CO at room temperature leads immediately to the quantitative formation of mononuclear dicarbonyl products as observed by infrared spectroscopy. In comparison, the related compound, $Cp_3Ir_3(CO)_3$, was found to react with ^{13}CO at 140 °C (refluxing xylene) forming $CpIr(^{13}CO)_2$, and the recovered $Cp_3Ir_3(CO)_3$ was unlabeled.[1h] While trinuclear clusters **1**–**4** also undergo bond scission in the presence of CO, the reaction is remarkably facile and occurs at much lower temperatures than observed for $Cp_3Ir_3(CO)_3$. Whether this is a direct function of weaker Ir–Ir bonding in **1** or a manifestation of the greater reactivity, especially in associative reactions, of indenyl vs cyclopentadienyl compounds[12] is not clear at present.

Experimental Section

General Procedures. All manipulations were conducted under an atmosphere of nitrogen with use of standard Schlenk techniques. (η^5-C$_9$H$_7$)Ir(η^2-C$_2$H$_4$)$_2$,[3] (η^5-C$_9$H$_7$)Ir(CO)$_2$,[3] and (η^5-C$_9$H$_7$)Rh(η^2-C$_2$H$_4$)$_2$[13] were prepared by literature methods. Preparative solvents were dried with use of standard methods and distilled. Deuterated solvents, $CDCl_3$ and CD_2Cl_2 (Cambridge Isotope Laboratories), for NMR studies were used as received.

^{1}H NMR spectra were recorded on a General Electric QE-300 spectrometer and were referenced to residual solvent resonances (7.26 ppm for $CDCl_3$ and 5.32 ppm for CD_2Cl_2). Infrared spectra were recorded on a Perkin-Elmer 1750 FT spectrophotometer. UV-visible spectra were recorded on a Hewlett-Packard HP8452A diode array spectrophotometer. Field-desorption (FD) mass spectra were recorded on a Finnigan-Mat 731 spectrometer by the staff of the Mass Spectrometry Laboratory of the School of Chemical Sciences. Microanalyses were performed by the staff of the Microanalytical Laboratory of the School of Chemical Sciences.

(η^5-C$_9$H$_7$)$_3$Ir$_3$(μ-CO)$_3$ (1). A yellow hexane solution (60 mL) of freshly generated (η^5-C$_9$H$_7$)Ir(CO)$_2$ (0.581 g, 1.60 mmol) in a 100 mL three-neck flask was purged with a stream of N_2 for 15 min and (η^5-C$_9$H$_7$)Ir(η^2-C$_2$H$_4$)$_2$ (0.581 g, 1.60 mmol) was added. The mixture was heated under reflux and stirred for 7 days, during which time the solution darkened and a red solid precipitated. The supernatant was removed via filter cannula, and the red solid was washed three times with *n*-hexane (20 mL) and three times with diethyl ether (20 mL) to remove remaining starting materials. Under these reaction conditions, only a trace of (η^5-C$_9$H$_7$)$_2$Ir$_2$(μ-CO)(CO)$_2$ (identified by its infrared spectrum[3]) was observed. The washings were combined and converted to (η^5-C$_9$H$_7$)Ir(CO)$_2$ under a stream of CO, resulting in a 23% recovery of the starting material as determined by infrared spectroscopy. The red solid was dried under vacuum: yield 797 mg (0.792 mmol, 74% conversion, 97% yield based on unrecovered starting material). X-ray quality crystals were formed by dissolving the red solid in a minimum amount of CH_2Cl_2 (5 mL) and layering with 2-propanol (30 mL). The red-orange crystals that formed overnight were collected by filtration, washed with 2-propanol (30 mL), and dried under vacuum: IR (ν_{CO}, CH_2Cl_2) 1809, 1763 cm^{-1}; IR (ν_{CO}, Nujol) 1786, 1751, 1731 cm^{-1}; FD-MS (100 °C) *m/z* (^{193}Ir) 1006 (η^5-C$_9$H$_7$)$_3$Ir$_3$(μ-CO)$_3^+$; UV-vis (CH_2Cl_2, $\lambda_{max}(\epsilon)$) 358 (15650); 528 (3080) nm. Anal. Calcd for $C_{30}H_{21}O_3Ir_3$: C, 35.81; H, 2.10. Found: C, 35.63; H, 2.13.

(η^5-C$_9$H$_7$)$_3$Ir$_{3-x}$Rh$_x$(μ-CO)$_3$ (1–4). A yellow hexane solution (30 mL) of freshly generated (η^5-C$_9$H$_7$)Ir(CO)$_2$ (100 mg, 0.275 mmol) in a 50 mL three-neck flask was purged with a stream of N_2 for 5 min and (η^5-C$_9$H$_7$)Rh(η^2-C$_2$H$_4$)$_2$ (76 mg, 0.275 mmol) was added. The mixture was heated under reflux and stirred for 48 h, during which time the solution darkened and

(9) (a) Shilling, B. E. R.; Hoffman, R. *J. Am. Chem. Soc.* **1979**, *101*, 3456. (b) Rives, A. B.; Xiao-Zeng, Y.; Fenske, R. F. *Inorg. Chem.* **1982**, *21*, 2286. (c) Trogler, W. C. *Acc. Chem. Res.* **1990**, *23*, 239.

(10) Delley, B.; Manning, M. C.; Ellis, D. E.; Berkowitz, J.; Trogler, W. C. *Inorg. Chem.* **1982**, *21*, 2247.

(11) Tyler, D. R.; Levenson, R. A.; Gray, H. B. *J. Am. Chem. Soc.* **1978**, *100*, 7888.

(12) (a) Rerek, M. E.; Basolo, F. *J. Am. Chem. Soc.* **1984**, *106*, 5908. (b) O'Connor, J. M.; Casey, C. P. *Chem. Rev.* **1987**, *87*, 307. (c) Szajek, L. P.; Shapley, J. R. *Organometallics* **1994**, *13*, 1395.

(13) Caddy, P.; Green, M.; O'Brien, E.; Smart, L. E.; Woodward, P. *J. Chem. Soc., Dalton Trans.* **1980**, 962.

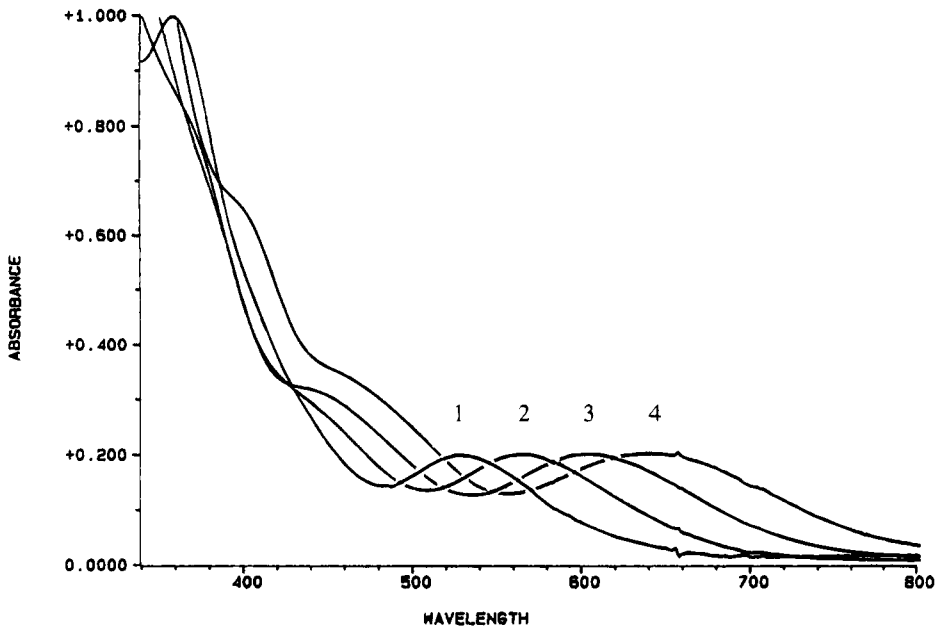

Figure 3.

precipitate was observed. The supernatant was removed via filter cannula, and the solid was washed three times with *n*-hexane (20 mL) and three times with diethyl ether (20 mL) to remove remaining starting materials. The remaining solid was dried under vacuum. The washings were combined and converted to $(\eta^5\text{-}C_9H_7)M(CO)_2$ (M = Rh, Ir) resulting in a 6.2% recovery of $(\eta^5\text{-}C_9H_7)Ir(CO)_2$ and 5.0% recovery of $(\eta^5\text{-}C_9H_7)$-$Rh(CO)_2$ as determined by infrared spectroscopy. The dark residue was dissolved in CH_2Cl_2 (10 mL) and placed on a 20 × 3 column of neutral alumina I (Aldrich) and eluted with CH_2-Cl_2. After the entire solution had been introduced onto the column, the mobile phase was changed to a 100:1 mixture of dichloromethane:acetone. The first green band yielded 6.9 mg of **4** (0.009 mmol) while the second green band gave 42.5 mg of **3** (0.051 mmol). The purple band gave 66.6 mg of **2** (0.073 mmol). Finally, elution with a 2:1 mixture of the same solvents provided 20.5 mg of red **1** (0.020 mmol). All four fractions were reduced in volume on a rotary evaporator and dried under vacuum. The clusters **1**–**4** were isolated in 2:7:5:1 molar ratios with 99% yield of Ir and 79% yield of Rh overall (incorporated into **1**–**4**) based on unrecovered starting materials: **1**, see above. **2**, IR (ν_{CO}, CH_2Cl_2) 1828, 1781, 1774 cm^{-1}; FD-MS (100 °C) *m/z* (^{193}Ir) 917 $(\eta^5\text{-}C_9H_7)_3Ir_2Rh(\mu\text{-}CO)_3^+$; UV-vis ($CH_2Cl_2$, $\lambda_{max}(\epsilon)$) 376sh (17230); 440sh (6830); 564 (4730) nm. Anal. Calcd for $C_{30}H_{21}O_3Ir_2Rh$: C, 39.30; H, 2.31. Found: C, 39.49; H, 2.42. **3**: IR (ν_{CO}, CH_2Cl_2) 1844, 1797 cm^{-1}; FD-MS (100 °C) *m/z* (^{193}Ir) 828 $(\eta^5\text{-}C_9H_7)_3IrRh_2(\mu\text{-}CO)_3^+$; UV-vis ($CH_2Cl_2$, $\lambda_{max}(\epsilon)$) 440sh (6620); 602 (4200) nm. Anal. Calcd for $C_{30}H_{21}O_3IrRh_2$: C, 43.54; H, 2.56. Found: C, 43.29; H, 2.61. **4**: IR (ν_{CO}, CH_2Cl_2) 1855, 1809 cm^{-1} (lit. 1852, 1805 cm^{-1})[1g,h]; FD-MS (100 °C) *m/z* (^{193}Ir) 738 $(\eta^5\text{-}C_9H_7)_3Rh_3(\mu\text{-}CO)_3^+$; UV-vis ($CH_2Cl_2$, λ_{max}) 400sh; 470; 636 nm.

Reactions of 1-4 with CO. A dark red CH_2Cl_2 solution of **1** was bubbled with CO for 5 min resulting in a yellow solution and a quantitative yield of $(\eta^5\text{-}C_9H_7)Ir(CO)_2$ as determined by infrared spectroscopy (ν_{CO}, CH_2Cl_2: 2035, 1971 cm^{-1}; lit.[3], light petroleum ether: 2042, 1980 cm^{-1}). The clusters **2**–**4** behave analogously under the same conditions, giving a mixture of $(\eta^5\text{-}C_9H_7)Ir(CO)_2$ and $(\eta^5\text{-}C_9H_7)Rh(CO)_2$ for the reaction with mixed metal clusters **2** and **3**, and only $(\eta^5\text{-}C_9H_7)Rh(CO)_2$ (ν_{CO}, CH_2Cl_2: 2044, 1984 cm^{-1}; lit.[1g,h], light petroleum ether: 2048, 1990 cm^{-1}) for the reaction with cluster **4**.

X-ray Structure Determination. Details are summarized in Table 2. The transparent red-orange platy data crystal had well-developed faces. Distances from the crystal center to the facial boundaries were 0.018, 0.010, and 0.19 mm, respectively. Diffraction data were collected at −50 °C. The structure of **1** was solved by using direct methods (SHELXS-86); correct positions for the Ir atoms were deduced from an E-map. Subsequent least-squares refinements and difference Fourier syntheses revealed positions for the remaining non-H atoms. H atoms were included in calculated positions. In the final cycle of least-squares refinement, non-H atoms were refined with anisotropic thermal coefficients, a common isotropic thermal parameter was refined for the H atoms, and an empirical isotropic extinction parameter converged to a small but significant value. The highest peaks in the final difference Fourier map were in the vicinity of the iridium atoms; the final map was broad but otherwise featureless. A final analysis of variance between observed and calculated structure factors revealed no systematic errors. The refined positional parameters are given in Table 3.

Acknowledgment. This research was supported by a grant from the National Science Foundation (CHE89-15349). M.C.C. thanks the Department of Chemistry for a fellowship funded by the Lubrizol Corp.

Supplementary Material Available: Tables of hydrogen atom coordinates, anisotropic thermal coefficients, a complete table of distances and angles, and van der Waals contacts (6 pages). Ordering information is given on any current masthead page.

OM940294V